

---

# Disentangling Redundancy for Multi-Task Pruning

---

**Xiaoxi He**  
ETH Zurich  
hex@ethz.ch

**Dawei Gao**  
Beihang University  
david\_gao@buaa.edu.cn

**Zimu Zhou\***  
ETH Zurich  
zzhou@tik.ee.ethz.ch

**Yongxin Tong**  
Beihang University  
yxtong@buaa.edu.cn

**Lothar Thiele**  
ETH Zurich  
thiele@ethz.ch

## Abstract

Can prior network pruning strategies eliminate redundancy in multiple correlated pre-trained deep neural networks? It seems a positive answer if multiple networks are first combined and then pruned. However, we argue that an arbitrarily combined network may lead to sub-optimal pruning performance because their intra- and inter-redundancy may not be minimised at the same time while retaining the inference accuracy in each task. In this paper, we define and analyse the redundancy in multi-task networks from an information theoretic perspective, and identify challenges for existing pruning methods to function effectively for multi-task pruning. We propose Redundancy-Disentangled Networks (RDNeTs), which decouples intra- and inter-redundancy such that all redundancy can be suppressed via previous network pruning schemes. A pruned RDNet also ensures minimal computation in any subset of tasks, a desirable feature for selective task execution. Moreover, a heuristic is devised to construct an RDNet from multiple pre-trained networks. Experiments on CelebA show that the same pruning method on an RDNet achieves at least  $1.8\times$  lower memory usage and  $1.4\times$  lower computation cost than on a multi-task network constructed by the state-of-the-art network merging scheme.

## 1 Introduction

Mobile applications continue to demand more functionalities on resource-constrained platforms. Examples include wearable cameras that recognise objects and identify people for the visually impaired, and drones that detect vehicles and identify road signs for traffic surveillance [6]. With deep neural networks well-trained for various tasks readily available [14, 20], a practical solution is to merge multiple individual-task models into a compact one by suppressing their redundancy [2, 9].

We investigate redundancy reduction in the context of *multi-task pruning*. Given multiple deep neural networks pre-trained for individual tasks, multi-task pruning aims to eliminate both *intra-redundancy* (due to over-parameterisation [4]) and *inter-redundancy* (due to task relatedness [2, 9]) so as to minimise the memory and computation cost when performing any subset of tasks at inference time. This objective also complies with the on-demand execution strategies common in mobile applications with frequently changing contexts and low resource budgets [17, 24].

An intuitive solution to multi-task pruning is to “combine & prune”. That is, first combine multiple networks by enforcing layer sharing among tasks and then squeeze the redundancy in the combined model via existing network pruning schemes. Such “combine & prune” seems plausible for two reasons: (i) Layer sharing among correlated tasks has recently been exploited to reduce the memory footprint of multiple pre-trained models [2, 9], and is a long-standing topic in multi-task learning

---

\*Corresponding Author: Zimu Zhou.

(MTL), which jointly learns multiple tasks to improve their generalisation [28]. (ii) The state-of-the-art pruning proposals [3, 5, 7] are able to radically lower the number of operations in an over-parameterised single-task network without loss in accuracy.

However, we argue that dedicated network merging schemes are compulsory if such “combine & prune” were to function in maximised synergy with single-task pruning. The challenge in pruning an arbitrarily combined multi-task network is that their intra- and inter-redundancy may not be minimised at the same time while retaining the inference accuracy in each task. For example, parameters redundant for one task may be necessary for another. Eliminating such parameters will reduce the redundancy in one task, but also decrease the inference accuracy in another task. Prior network merging research focuses on different objectives such as overall memory consumption [2, 9] and task generalisation [23, 28]. None of them has explored whether the combined network can be further condensed effectively by existing single-task pruning methods.

In this paper, we take an information theoretic perspective on multi-task pruning, and analyse conditions for single-network pruning methods to be able to suppress redundancy both within and across tasks in a combined model. We also propose a heuristic that constructs such a network from multiple pre-trained single-task neural network. Our main contributions and results are as follows:

- We define and analyse inter- and intra-redundancy from an information theoretic perspective, and show that simultaneously reducing inter- and intra-redundancy without accuracy loss in tasks may be conflicting. Such a conflict poses challenges for existing network pruning methods to effectively function in multi-task pruning. To the best of our knowledge, this is the first exploration on applying single-task pruning methods to multi-task pruning.
- We propose Redundancy-Disentangled Networks (RDNeTs), which minimise the conflict and enable suppressing both intra- and inter-redundancy via single-task pruning. We also design a heuristic network merging scheme to construct an RDNet from pre-trained networks. Experiments on CelebA [16] (LFW [11]) dataset show that applying the same single-task pruning method on an RDNet achieves at least  $1.8\times$  ( $1.3\times$ ) lower memory usage and  $1.4\times$  ( $1.8\times$ ) lower computation cost than on a multi-task network constructed by the state-of-the-art network merging scheme [9].

## 2 Related Work

**Single-Task Pruning.** Network pruning is the de facto approach to reduce the number of operations in a deep neural network without incurring loss in accuracy [21]. Unstructured pruning reduces the redundancy in a network by eliminating the unimportant weights [5, 7]. However, customized hardware [8] is compulsory to exploit such irregular sparse connections for inference acceleration. Alternatively, structured pruning enforces sparsity at the granularity of channels/filters [15, 26] or neurons [3, 10]. The resulting sparsity is more regular and easier to achieve acceleration on general-purpose mobile processors.

All previous network pruning research deals with the *intra-redundancy* of a single network. We make the first attempt to enable prior single-task pruning strategies for multi-task pruning such that both *intra-* and *inter-redundancy* of correlated tasks can be suppressed. Aimed at multi-task inference acceleration on general-purpose processors, we enforce neuron-level sparsity within networks as [3, 10] and a higher-level regular sparsity across networks, as will be shown in Sec. 3.3.

**Multi-Task Networks.** Multi-Task Learning (MTL) is a paradigm that often jointly trains multiple correlated tasks from scratch for better generalisation of tasks [28]. In MTL, a multi-task network is typically configured to avoid improper knowledge transfer [27]. Our work differs from general MTL in that the latter seldom account for the compactness of a multi-task network or any subset of tasks therein. Furthermore, most MTL proposals ignore models pre-trained for individual tasks.

Few proposals have explored constructing a compact multi-task network from pre-trained models [2, 9, 23]. Vandenhende *et al.* propose a branched multi-task structure by analysing the task relatedness among pre-trained networks, which implicitly reduces their overall size. MTZ [9] and NeuralMerger [2] explicitly compress inter-redundancy by weight sharing among pre-trained networks to reduce their overall memory footprint. In addition to decreasing memory consumption, we also aim at a multi-task network with minimal computation workload. Moreover, we study analytically and empirically whether intra- and inter-redundancy can be simultaneously eliminated by single-task pruning, a problem unexplored in prior research [2, 9, 23].

### 3 Redundancy-Disentangled Networks for Multi-Task Pruning

In this section, we study the redundancy of neural networks in the context of multi-task pruning and propose Redundancy-Disentangled Networks (RDNeTs), which enable prior single-task pruning strategies to function effectively in multi-task pruning. We first present an intuition on the entangled redundancy in a multi-task pruning in Sec. 3.1. Then we formally define the problem and identify conditions for disentangled redundancy in Sec. 3.2. Finally we design a heuristic to construct an RDNet in Sec. 3.3. For ease of presentation, all the analysis and solution are explained using two neural networks. We discuss extensions to multiple (more than two) neural networks in Sec. 3.4.

#### 3.1 Entangled Redundancy: An Intuition

Assume we have two pre-trained neural networks for two tasks  $A$  and  $B$ . Our goal is to combine them into a multi-task network and apply existing single-task pruning schemes on the combined network to reduce its redundancy.

Neural networks extract and process information from its input. Intuitively there is information only relevant to task  $A$ , which we call *task- $A$ -exclusive information*. Similarly, there is *task- $B$ -exclusive information*. Moreover, if task  $A$  and  $B$  are correlated, there should be *task-shared information* that is relevant to both tasks. Consider a joint multi-task network architecture with two output layers for task  $A$  and  $B$ . It can be divided into three parts: a *task- $A$ -exclusive sub-network* which connects only to output  $A$ , a *task- $B$ -exclusive sub-network* which connects only to output  $B$ , and a *shared sub-network* which connects to both outputs. An arbitrary multi-task network architecture may encounter the following problems when applying single-task pruning for redundancy reduction.

- If the task- $A$ -exclusive sub-network and the task- $B$ -exclusive sub-network contain some task-shared information, such information may be necessary for both tasks and hence will not be removed via single-task pruning on each task. However, such task-shared information is redundant because it is duplicated in the joint multi-task network. Hence, in this case, single-task pruning cannot reduce all redundancy in a multi-task network.
- If the shared sub-network contains task-exclusive information which is not captured by the two task-exclusive networks, such information is necessary for one task but is redundant for another. Performing single-task pruning on one task may remove important information for another task, thus decreasing its inference accuracy.

The above example calls for a deeper understanding on the redundancy within and across tasks and its impact on multi-task pruning, as we will explain next.

#### 3.2 Analysis on Redundancy in Multi-Task Pruning

Our analysis leverages recent advances in information theoretic perspectives on deep learning [19, 22]. We first define redundancy reducible in single-task pruning and multi-task pruning, respectively. We then point out the problem of redundancy entanglement and finally identify the conditions of disentangled redundancy for multi-task pruning.

**Graph Representation of Neural Networks.** Consider three sets of random variable  $\mathbf{X} \in \mathcal{X}$ ,  $\mathbf{Y}^A \in \mathcal{Y}^A$ , and  $\mathbf{Y}^B \in \mathcal{Y}^B$ . A task  $t$  is defined as finding the conditional distribution  $\Pr(\mathbf{Y}^t = \mathbf{y} | \mathbf{X} = \mathbf{x})$ , with  $t = A$  or  $B$ . The architecture of a neural network  $M$  without loop can be described as a simple acyclic directed graph  $G = (V, E)$ , with a vertex set  $V$  and an edge set  $E$ . The *inputs* of a vertex is the *outputs* of all its in-coming neighbours. The vertex set  $V$  contains sink, source and internal nodes, which are defined in Appendix A.1 (in supplementary material). As an example, two separately pre-trained neural networks  $M^A$  and  $M^B$  can be represented jointly in a graph  $G^{A,B}$  in Fig. 1 (a).

Two vertices  $v_1$  and  $v_2$  in a neural graph  $G$  are said to be *connected*, if there exists a path from  $v_1$  to  $v_2$  or vice-versa. Otherwise,  $v_1$  and  $v_2$  are said to be *unconnected*. A graph  $G^A$  is said to be *task- $A$ -connected* iff. all internal node  $v_i \in G^A$  are connected with  $v^A$ .

We can organise a neural graph  $G$  into layers  $\Gamma_i$  by Algorithm 2 in Appendix A.2. The output set of neurons in  $\Gamma_i$  is called *layer output*, denoted by  $\mathbf{L}_i$ . It is easy to see that in a task- $A$ -connected graph, the layer outputs form a Markov chain [22]:

$$\mathbf{Y}^A \rightarrow \mathbf{L}_0^A \rightarrow \mathbf{L}_1^A \rightarrow \dots \rightarrow \mathbf{L}_N^A \rightarrow \mathbf{L}_{N+1}^A \quad (1)$$

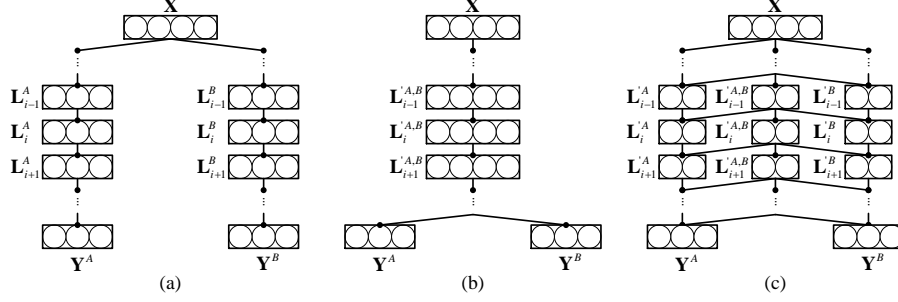


Figure 1: (a) Two separately pre-trained neural network for each task. (b) A simple feed-forward multi-task network without task-exclusive sub-graph. (c) An RDNet constructed by Algorithm 1. Notice that the edges in the figures mean fully connection between neuron blocks.

where  $L_0^A = X$  and  $L_{N+1}^A = \hat{Y}^A$ .

To simplify the notation, for a neuron output  $T_i$ , we write  $T_i \in G$  when its corresponding vertex  $v_i$  is in  $G$ . For a set of neuron outputs  $\mathbf{T}$ , we write  $\mathbf{T} \in G$  when its all corresponding vertices are in  $G$ .

**Redundancy in Single-Task Pruning.** We define the redundancy in a neural network from the perspective of information theory:

**Definition 3.1.** The *redundancy* of a set of neuron outputs  $\mathbf{T}$  with regard to task  $A$  is the amount of information that the outputs would contain if they were totally independent of one another, minus the amount of task- $A$ -relevant information that they actually possess. This can be measured by  $\mathcal{R}_A(\mathbf{T}) = \sum_{T_i \in \mathbf{T}} H(T_i) - I(\mathbf{T}; Y^A)$ .

By this definition we have

$$\mathcal{R}_A(\mathbf{T}) = \sum_{T_i \in \mathbf{T}} H(T_i) - \left( H(\mathbf{T}) - H(\mathbf{T}|Y^A) \right) = C(\mathbf{T}) + H(\mathbf{T}|Y^A) \quad (2)$$

where  $C(\mathbf{T}) = \sum_{T_i \in \mathbf{T}} H(T_i) - H(\mathbf{T})$  is the *total correlation* [25]. Eq.(2) can be interpreted as: the task-related redundancy within a neuron output set consists of the self-redundancy, measured by  $C(\mathbf{T})$ , and the unnecessary information for the task, measured by  $H(\mathbf{T}|Y^A)$ . Notice that  $\mathcal{R}_A(\mathbf{T}) \geq 0$  for any  $A$  and  $\mathbf{T}$ .

As shown in [19, 22], the inference accuracy of a neural network  $M^A$  is positively correlated to the task-related information transmitted through the network, measured by  $\sum_{i=1}^N I(L_i; Y^A)$ . Hence pruning can be understood as minimising the the redundancy w.r.t. the task within the network to reduce its memory and computation cost while preserving its inference accuracy. This can be formalised as an optimisation problem (for simplicity we write  $\mathcal{R}_A(\{T|T \in G^A\})$  as  $\mathcal{R}_A(G^A)$ ):

$$\text{minimise } \mathcal{R}_A(G^A) - \xi \cdot \sum_{i=1}^N I(L_i^A; Y^A) \quad (3)$$

where  $\xi$  is a parameter to control the trade-off between inference accuracy and inference efficiency.

It is however more convenient to analyse the redundancy *layer-by-layer*. In general, the redundancy of the join of two neuron output sets  $\mathbf{T}^1$  and  $\mathbf{T}^2$  can be calculated by (derivation in Appendix A.3):

$$\mathcal{R}_A(\mathbf{T}^1 \cup \mathbf{T}^2) = \mathcal{R}_A(\mathbf{T}^1) + \mathcal{R}_A(\mathbf{T}^2) + I(\mathbf{T}^1; \mathbf{T}^2; Y^A) - \sum_{T_i \in \mathbf{T}^1 \cap \mathbf{T}^2} H(T_i) \quad (4)$$

where  $I(\mathbf{T}^1; \mathbf{T}^2; Y^A) = I(\mathbf{T}^1; \mathbf{T}^2) - I(\mathbf{T}^1; \mathbf{T}^2|Y^A)$  is the *co-information* [1]. From Eq.(4), we have (derivation in Appendix A.4):

$$\mathcal{R}_A(G^A) = \sum_{i=1}^N \left( \mathcal{R}_A(L_i^A) - \sum_{T_i \in L_{i-1}^A \cap L_i^A} H(T_i) \right) + \sum_{i=2}^N I(L_i^A; Y^A) \quad (5)$$

Hence the single-task pruning problem in Eq.(3) has an equivalent layer-wise formulation (with different tuning-parameter  $\xi_i$ ):

$$\text{minimise } \sum_{i=1}^N \left( \mathcal{R}_A(\mathbf{L}_i^A) - \sum_{T_i \in \mathbf{L}_{i-1}^A \cap \mathbf{L}_i^A} H(T_i) - \xi_i \cdot I(\mathbf{L}_i^A, \mathbf{Y}^A) \right) \quad (6)$$

**Redundancy in Multi-Task Pruning.** Now consider a joint graph  $G^{A,B}$  for task  $A$  and  $B$ . It contains a task- $A$ -connected graph  $G^A$  and a task- $B$ -connected graph  $G^B$ . It also contains a task- $A$ -exclusive graph defined as  $G'^A = G^A \setminus G^B$ , a task- $B$ -exclusive graph defined as  $G'^B = G^B \setminus G^A$ , and a task- $A,B$ -shared graph defined as  $G'^{A,B} = G^A \cap G^B$ . Also for any layer output  $\mathbf{L} \in G^{A,B}$ , its contained neuron outputs can be organised into task- $A$ -connected  $\mathbf{L}^A = \{T|T \in G^A \wedge T \in \mathbf{L}\}$ , task- $B$ -connected  $\mathbf{L}^B = \{T|T \in G^B \wedge T \in \mathbf{L}\}$ , task- $A$ -exclusive  $\mathbf{L}'^A = \{T|T \in G'^A \wedge T \in \mathbf{L}\}$ , task- $B$ -exclusive  $\mathbf{L}'^B = \{T|T \in G'^B \wedge T \in \mathbf{L}\}$ , and task- $A,B$ -shared  $\mathbf{L}'^{A,B} = \{T|T \in G'^{A,B} \wedge T \in \mathbf{L}\}$ . Notice that  $\mathbf{L}^A = \{\mathbf{L}'^A, \mathbf{L}'^{A,B}\}$  and  $\mathbf{L}^B = \{\mathbf{L}'^B, \mathbf{L}'^{A,B}\}$ .

Now we can define the intra- and inter-redundancy in a joint graph  $G^{A,B}$ :

**Definition 3.2.** The *intra-redundancy* of  $G^{A,B}$  w.r.t. task  $A$  is defined as the redundancy of all task- $A$ -connected neuron outputs w.r.t. task  $A$

$$R_{intra}^A = \mathcal{R}_A(G^A) \quad (7)$$

**Definition 3.3.** The *inter-redundancy* of  $G^{A,B}$  between  $A$  and  $B$  is the sum of mutual information between all task- $A$ -exclusive neuron outputs and all task- $B$ -exclusive neuron outputs in each layer.

$$R_{inter}^{A,B} = \sum_{i=1}^N I(\mathbf{L}_i'^A; \mathbf{L}_i'^B) \quad (8)$$

Reducing the intra-redundancy will improve inference efficiency when only one task is performed. Reducing  $R_{inter}^{A,B}$  will improve inference efficiency when both tasks are performed.

Similar to Eq.(6), multi-task pruning can be formulated as a multi-objective optimisation problem:

$$\begin{aligned} \text{minimise } & \sum_{i=1}^N \left( \mathcal{R}_A(\mathbf{L}_i^A) - \sum_{T_i \in \mathbf{L}_{i-1}^A \cap \mathbf{L}_i^A} H(T_i) - \xi_i^A \cdot I(\mathbf{L}_i^A; \mathbf{Y}^A) \right), \\ & \sum_{i=1}^N \left( \mathcal{R}_B(\mathbf{L}_i^B) - \sum_{T_i \in \mathbf{L}_{i-1}^B \cap \mathbf{L}_i^B} H(T_i) - \xi_i^B \cdot I(\mathbf{L}_i^B; \mathbf{Y}^B) \right), \\ & \sum_{i=1}^N I(\mathbf{L}_i'^A; \mathbf{L}_i'^B) \end{aligned} \quad (9)$$

Minimising these objective functions results in minimal computation and memory cost when both tasks are performed concurrently as well as when each task is performed individually.

**Entangled and Disentangled Redundancy.** Applying prior single-task pruning methods on an arbitrary joint graph  $G^{A,B}$  encounters the problem of entangled redundancy. This is because the multi-objective optimisation problem in Eq.(9) on  $G^{A,B}$  is non-trivial.

- The first two objective conflict with each other because the existence of necessary task-exclusive information in  $\mathbf{L}$ , which can be measured by  $I(\mathbf{L}_i'^{A,B}; \mathbf{Y}^A | \mathbf{L}_i'^A, \mathbf{Y}^B)$  and  $I(\mathbf{L}_i'^{A,B}; \mathbf{Y}^B | \mathbf{L}_i'^B, \mathbf{Y}^A)$ . Reducing  $\mathcal{R}_A(\mathbf{L}_i^A)$  may decrease  $I(\mathbf{L}_i'^{A,B}; \mathbf{Y}^A | \mathbf{L}_i'^A, \mathbf{Y}^B)$ , but also decrease  $I(\mathbf{L}_i'^B; \mathbf{Y}^B)$ , and hence increases the second objective.
- The first and second objectives also conflict with the third, if there is shared information duplicated in  $\mathbf{L}_i'^A$  and  $\mathbf{L}_i'^B$ , which can be measured by  $I(\mathbf{L}_i'^A; \mathbf{L}_i'^B; \mathbf{Y}^A; \mathbf{Y}^B)$ . Reducing  $R_{inter}^{A,B}$  may eliminate such information, yet decrease  $I(\mathbf{L}_i^A; \mathbf{Y}^A)$  or  $I(\mathbf{L}_i^B; \mathbf{Y}^B)$ .

Our key observation here is that enforcing  $I(\mathbf{L}_i^{A,B}; \mathbf{L}_i^{A,B}; \mathbf{Y}^A; \mathbf{Y}^B)$ ,  $I(\mathbf{L}_i^{A,B}; \mathbf{Y}^A | \mathbf{L}_i^A, \mathbf{Y}^B)$ , and  $I(\mathbf{L}_i^{A,B}; \mathbf{Y}^B | \mathbf{L}_i^B, \mathbf{Y}^A)$  to be zero will disentangle the redundancy. If  $I(\mathbf{L}_i^{A,B}; \mathbf{L}_i^{A,B}; \mathbf{Y}^A; \mathbf{Y}^B) = 0$ , the first two objective in (9) will no longer conflict with the third. Moreover, we have  $I(\mathbf{L}_i^{A,B}; \mathbf{L}_i^{A,B}) = I(\mathbf{L}_i^{A,B}; \mathbf{L}_i^{A,B}; \mathbf{Y}^A; \mathbf{Y}^B) + I(\mathbf{L}_i^{A,B}; \mathbf{L}_i^{A,B}; \mathbf{Y}^A | \mathbf{Y}^B) + I(\mathbf{L}_i^{A,B}; \mathbf{L}_i^{A,B}; \mathbf{Y}^B | \mathbf{Y}^A) + I(\mathbf{L}_i^{A,B}; \mathbf{L}_i^{A,B} | \mathbf{Y}^A, \mathbf{Y}^B)$ . The term  $I(\mathbf{L}_i^{A,B}; \mathbf{L}_i^{A,B}; \mathbf{Y}^A | \mathbf{Y}^B)$  can be interpreted as the task-A-exclusive information duplicated in the task-exclusive neurons. This is reduced together with  $\mathcal{R}_B(\mathbf{L}_i^B)$  since it is irrelevant information for  $B$ . The term  $I(\mathbf{L}_i^{A,B}; \mathbf{L}_i^{A,B}; \mathbf{Y}^B | \mathbf{Y}^A)$  can also be reduced together with  $\mathcal{R}_A(\mathbf{L}_i^A)$  in the same way. The last term  $I(\mathbf{L}_i^{A,B}; \mathbf{L}_i^{A,B} | \mathbf{Y}^A, \mathbf{Y}^B)$  can be interpreted as the duplicated information irrelevant to either  $A$  or  $B$ . Such information can be eliminated together with  $\mathcal{R}_A(\mathbf{L}_i^A)$  or  $\mathcal{R}_B(\mathbf{L}_i^B)$ . Thus when  $I(\mathbf{L}_i^{A,B}; \mathbf{L}_i^{A,B}; \mathbf{Y}^A; \mathbf{Y}^B) = 0$ , the inter-redundancy can be eliminated by minimising the intra-redundancy. Then the optimisation problem in Eq.(9) is reduced to:

$$\begin{aligned} \text{minimise} \quad & \sum_{i=1}^N \left( \mathcal{R}_A(\mathbf{L}_i^A) - \sum_{T_i \in \mathbf{L}_{i-1}^A \cap \mathbf{L}_i^A} H(T_i) - \xi_i^A \cdot I(\mathbf{L}_i^A; \mathbf{Y}^A) \right), \\ & \sum_{i=1}^N \left( \mathcal{R}_B(\mathbf{L}_i^B) - \sum_{T_i \in \mathbf{L}_{i-1}^B \cap \mathbf{L}_i^B} H(T_i) - \xi_i^B \cdot I(\mathbf{L}_i^B; \mathbf{Y}^B) \right) \quad (10) \\ \text{s.t.} \quad & \forall i = 1, \dots, N, I(\mathbf{L}_i^{A,B}; \mathbf{L}_i^{A,B}; \mathbf{Y}^A; \mathbf{Y}^B) = 0 \end{aligned}$$

If  $I(\mathbf{L}_i^{A,B}; \mathbf{Y}^A | \mathbf{L}_i^A, \mathbf{Y}^B) = I(\mathbf{L}_i^{A,B}; \mathbf{Y}^B | \mathbf{L}_i^B, \mathbf{Y}^A) = 0$  holds for all  $i = 1, \dots, N$ , the multi-objective optimisation problem in Eq.(10) becomes trivial as the objectives are no longer conflicted.

In summary, the inter- and intra-redundancy in a multi-task network can be minimised with single-task pruning methods, if the network satisfies the property that  $I(\mathbf{L}_i^{A,B}; \mathbf{L}_i^{A,B}; \mathbf{Y}^A; \mathbf{Y}^B) = I(\mathbf{L}_i^{A,B}; \mathbf{Y}^A | \mathbf{L}_i^A, \mathbf{Y}^B) = I(\mathbf{L}_i^{A,B}; \mathbf{Y}^B | \mathbf{L}_i^B, \mathbf{Y}^A) = 0$  at each layer  $L_i$ . We call such a network *Redundancy-Disentangled Network (RDNet)*. Hence, to address multi-task pruning problem with “combine & prune” scheme, we propose to first merge the pre-trained networks into an RDNet.

### 3.3 Constructing Redundancy-Disentangled-Networks

We propose a heuristic to construct an RDNet from pre-trained single-task networks. For two simple feed-forward network  $M^A$  with  $N^A$  layers and  $M^B$  with  $N^B$  layers, we align their layers from the first one. For each layer  $i = 1, \dots, N^{A,B}$  with  $N^{A,B} = \min\{N^A, N^B\}$ , we find a set of neurons such that  $I(\mathbf{T}_i^A; \mathbf{Y}^B) \approx 0$  and a set  $I(\mathbf{T}_i^B; \mathbf{Y}^A) \approx 0$ . Then the set  $\mathbf{T}_i^{A \cap B}$  contains the remaining neurons. Accordingly, we have three sets of neurons within each layer:  $\mathbf{T}_i^A$ ,  $\mathbf{T}_i^B$  and  $\mathbf{T}_i^{A \cap B}$ .

To find  $I(\mathbf{T}_i^A; \mathbf{Y}^B) \approx 0$  and  $I(\mathbf{T}_i^B; \mathbf{Y}^A) \approx 0$ , we use a greedy-search method: at the  $i$ -th layer  $\mathbf{L}_i$ , we start by choosing a neuron  $T_{i,j}$  such that  $I(T_{i,j}; \mathbf{Y}^B) < \alpha$  as the first element in  $\mathbf{T}_i^A$ . Then we iteratively add new  $T_{i,j}$  into  $\mathbf{T}_i^A$  such that  $I(\mathbf{T}_i^A; \mathbf{Y}^B) < \alpha$ . Since the mutual information is numerically estimated, it is impossible to be exactly 0. Therefore we use a threshold parameter  $\alpha$ .

Then we reconstruct the connections between each layer. The edges  $\mathbf{T}_{i-1}^B \rightarrow \mathbf{T}_i^A$  and  $\mathbf{T}_{i-1}^A \rightarrow \mathbf{T}_i^B$  are unnecessary because  $I(\mathbf{T}_{i-1}^B; \mathbf{T}_i^A; \mathbf{Y}^A) \leq I(\mathbf{T}_{i-1}^B; \mathbf{Y}^A) \approx 0$  and  $I(\mathbf{T}_{i-1}^A; \mathbf{T}_i^B; \mathbf{Y}^B) \leq I(\mathbf{T}_{i-1}^A; \mathbf{Y}^B) \approx 0$ . We also disconnect the edges  $\mathbf{T}_{i-1}^B \rightarrow \mathbf{T}_i^{A \cap B}$  and  $\mathbf{T}_{i-1}^A \rightarrow \mathbf{T}_i^{A \cap B}$ , so that  $\mathbf{T}_i^A$  and  $\mathbf{T}_i^B$  become task-exclusive.

The remaining connections are  $\mathbf{T}_{i-1}^A \rightarrow \mathbf{T}_i^A$ ,  $\mathbf{T}_{i-1}^B \rightarrow \mathbf{T}_i^B$ , and  $\mathbf{T}_{i-1}^{A,B} \rightarrow \mathbf{T}_i^{A,B}$ . They will maintain their original weights, or in case that they do not exist in the pre-trained single-task networks, receive an initialised weight (zero or random value near zero). We use  $I(\mathbf{T}_i^A; \mathbf{Y}^B) \approx 0$  and  $I(\mathbf{T}_i^B; \mathbf{Y}^A) \approx 0$  to approximate  $I(\mathbf{L}_i^{A,B}; \mathbf{L}_i^{A,B}; \mathbf{Y}^A; \mathbf{Y}^B) = 0$ . By removing task-exclusive neurons from  $\mathbf{T}_i^{A \cap B}$ ,  $I(\mathbf{L}_i^{A,B}; \mathbf{Y}^A | \mathbf{L}_i^A, \mathbf{Y}^B)$  and  $I(\mathbf{L}_i^{A,B}; \mathbf{Y}^B | \mathbf{L}_i^B, \mathbf{Y}^A)$  are also reduced.

Algorithm 1 illustrates the heuristic to construct an RDNet from two pre-trained single-task neural networks. The result topology is shown in Fig. 1 (c).

---

**Algorithm 1:** Merging two neural networks into an RDNet.

---

**Input:** Pre-trained networks  $M^A$  and  $M^B$  with aligned layer outputs  $\mathbf{L}_i^A$  and  $\mathbf{L}_i^B$ ,  $\mathbf{Y}^A$ ,  $\mathbf{Y}^B$ , threshold parameter  $\alpha$

**Output:** joint model  $M^{A,B}$

```
1 for  $i \leftarrow 1$  to  $\min\{N^A, N^B\}$  do
2    $\mathbf{F}^A \leftarrow \mathbf{F}^B \leftarrow \mathbf{T}'^{A \cap B} \leftarrow \{\mathbf{T}_i^A, \mathbf{T}_i^B\}$ ;
3    $\mathbf{T}'^A \leftarrow \arg \min_{T_{i,j}^A \in \mathbf{F}^A} I(T_{i,j}^A; \mathbf{Y}^B)$ ;
4    $\mathbf{F}^A \leftarrow \mathbf{F}^A \setminus \mathbf{T}'^A$ ;
5   while  $I(\mathbf{T}'^A; \mathbf{Y}^B) \leq \alpha$  do
6      $T^A \leftarrow \arg \min_{T_{i,j}^A \in \mathbf{F}^A} I(\{T_{i,j}^A, \mathbf{T}'^A\}; \mathbf{Y}^B)$ ;
7      $\mathbf{F}^A \leftarrow \mathbf{F}^A \setminus \{T^A\}$ ;
8      $\mathbf{T}'^A \leftarrow \mathbf{T}'^A \cup \{T^A\}$ ;
9   end
10   $\mathbf{T}'^B \leftarrow \arg \min_{T_{i,j}^B \in \mathbf{F}^B} I(T_{i,j}^B; \mathbf{Y}^A)$ ;
11   $\mathbf{F}^B \leftarrow \mathbf{F}^B \setminus \mathbf{T}'^B$ ;
12  while  $I(\mathbf{T}'^B; \mathbf{Y}^A) \leq \alpha$  do
13     $T^B \leftarrow \arg \min_{T_{i,j}^B \in \mathbf{F}^B} I(\{T_{i,j}^B, \mathbf{T}'^B\}; \mathbf{Y}^A)$ ;
14     $\mathbf{F}^B \leftarrow \mathbf{F}^B \setminus \{T^B\}$ ;
15     $\mathbf{T}'^B \leftarrow \mathbf{T}'^B \cup \{T^B\}$ ;
16  end
17   $\mathbf{T}'^{A \cap B} \leftarrow \mathbf{T}'^{A \cap B} \setminus (\mathbf{T}'^A \cup \mathbf{T}'^B)$ ;
18   $\mathbf{T}_{tmp} \leftarrow \mathbf{T}'^A \cap \mathbf{T}'^B$ ;
19   $\mathbf{T}'^A \leftarrow \mathbf{T}'^A \setminus \mathbf{T}_{tmp}$ ;
20   $\mathbf{T}'^B \leftarrow \mathbf{T}'^B \setminus \mathbf{T}_{tmp}$ ;
21  Connect  $\mathbf{T}'_{i-1}^A \rightarrow \mathbf{T}'_i^A$ ,  $\mathbf{T}'_{i-1}^B \rightarrow \mathbf{T}'_i^B$ , and  $\mathbf{T}'_{i-1}^{A,B} \rightarrow \mathbf{T}'_i^{A,B}$ ;
22 end
```

---

### 3.4 Extension to Three or More Tasks

When there are  $K \geq 3$  tasks, we define the set of all the task as  $v = \{t_1, \dots, t_K\}$ . The joint network can be divided into *subset- $\tau$ -exclusive* sub-graphs  $G'^\tau$ , where  $\tau \subseteq v$  and  $\tau \neq \emptyset$ . Each neuron in  $G'^\tau$  connects to all the outputs  $\mathbf{Y}^t$  with  $t \in \tau$ . Also, we define  $\mathbf{Y}^\tau = \{\mathbf{Y}^t | t \in \tau\}$ .

Then the condition for an RDNet is extended to

$$\begin{aligned} \forall i = 1, \dots, N \text{ and } \tau_A \neq \tau_B, \quad & I(\mathbf{L}_i^{\tau_A}; \mathbf{L}_i^{\tau_B}; \mathbf{Y}^{\tau_A}; \mathbf{Y}^{\tau_B}) = 0 \\ & I(\mathbf{L}_i^{\tau_A \cup \tau_B}; \mathbf{Y}^{\tau_A} | \mathbf{L}_i^{\tau_A}, \mathbf{Y}^{\tau_B}) = 0 \\ & I(\mathbf{L}_i^{\tau_A \cup \tau_B}; \mathbf{Y}^{\tau_B} | \mathbf{L}_i^{\tau_B}, \mathbf{Y}^{\tau_A}) = 0 \end{aligned} \quad (11)$$

The heuristic method to construct RDNet also needs to be extended: now we use the same greedy-search method to find subset-exclusive neurons  $\mathbf{T}'_i^\tau$  in each layer, such that  $I(\mathbf{T}'_i^\tau; \mathbf{Y}^{v \setminus \tau}) \approx 0$ . And we connect  $\mathbf{T}'_{i-1}^{\tau_1} \rightarrow \mathbf{T}'_i^{\tau_2}$  only when  $\tau_2 \subseteq \tau_1$ .

## 4 Experiments

Since there is no existing dedicated multi-task network design to facilitate single-task network pruning, we compare the performance of the following merging schemes for multi-task pruning.

- **Baseline 1.** A pseudo joint network consisting of two separated single-task network as in Fig. 1 (a). The intra-redundancy in this joint network can be efficiently reduced with single-task pruning methods. However, the inter-redundancy cannot be eliminated.
- **Baseline 2.** A joint network constructed via MTZ, the state-of-the-art network merging scheme for cross-model memory cost compression [9]. We use MTZ to fully merge the

Table 1: Test accuracy, number of parameters, and MFLOPs on CelebA

Task	Accuracy			#Parameters ( $\times 10^5$ )			MFLOPs		
	<i>A</i>	<i>B</i>	<i>A&amp;B</i>	<i>A</i>	<i>B</i>	<i>A&amp;B</i>	<i>A</i>	<i>B</i>	<i>A&amp;B</i>
Baseline 1	89.54%	88.08%	88.81%	3.28	3.05	6.34	8.85	11.33	20.18
Baseline 2	89.36%	87.78%	88.57%	4.45	4.45	4.45	13.89	13.89	13.89
RDNet	89.37%	87.89%	88.63%	2.37	2.06	2.51	9.76	9.82	9.90

Table 2: Test accuracy, number of parameters, and MFLOPs on LFW

Task	Accuracy			#Parameters ( $\times 10^5$ )			MFLOPs		
	<i>A</i>	<i>B</i>	<i>A&amp;B</i>	<i>A</i>	<i>B</i>	<i>A&amp;B</i>	<i>A</i>	<i>B</i>	<i>A&amp;B</i>
Baseline 1	89.03%	81.29%	85.16%	1.39	2.24	3.63	2.70	4.19	6.89
Baseline 2	88.89%	80.90%	84.89%	2.70	2.70	2.70	5.62	5.62	5.62
RDNet	88.70%	80.96%	84.83%	1.84	1.89	2.11	3.07	3.08	3.16

smaller network “into” the larger one such that the joint network also saves computation cost (Fig. 1 (b)). By definition, there is no inter-redundancy in such a joint network. However the absence of task-exclusive graphs means that the intra-redundancy cannot be fully reduced simultaneously. Moreover, the conflict between the first two terms in Eq.(9) may cause sub-optimal pruning results.

- **RDNet.** An RDNet constructed by Algorithm 2 as illustrated in Fig. 1 (c). We use a KL-based mutual information upper bound estimator from [12].

We prune the multi-task networks in the two baselines and an RDNet with Variational Information Bottleneck (VIB) [3]. VIB explicitly reduces the amount of information in each layer and offers the state-of-the-art pruning performance. It is also a structured pruning method which can accelerate the inference without customised hardware support.

We assess the performance of different methods with memory usage (measured by number of parameters) and computation cost (measured by FLOPs) of the pruned multi-task networks.

All experiments are implemented with TensorFlow and conducted on a workstation equipped with Nvidia RTX 2080 Ti GPU.

#### 4.1 VGG-16 on CelebA

**Dataset and Settings.** This experiment is conducted on the CelebA dataset [16] with VGG-16 architecture [20]. CelebA contains over 200 thousand celebrity face images labelled with 40 attributes. We divide the 40 attributes into two groups (20/20) to form task *A* and *B*. More implementation details can be found in Appendix B.1.

**Results.** Table 1 summarises the performance evaluation of the baselines and RDNet on CelebA. RDNet achieves in general better performance in terms of memory usage and computation cost compared with baseline 1 and 2. Especially, RDNet achieves at least  $1.8\times$  lower memory usage and  $1.4\times$  lower computation cost in comparison to baseline 2.

#### 4.2 VGG-16 on LFW

**Dataset and Settings.** This experiment is conducted on the Labeled Faces in the Wild (LFW) dataset [11]. The LFW dataset contains over 13,000 face photographs collected from the web. Each face photo is associated with 75 attributes [13]. We choose 20 of them to form task *A*, and another 20 to form task *B*. The detailed implementation settings can be found in Appendix B.2

**Results.** Table 2 summarises the performance evaluation on LFW. It shows similar results as in Sec. 4.1, that RDNet achieves lower memory usage and computation cost in general.



## 5 Conclusion

In this paper, we define and analyse the redundancy in multi-task networks from an information theoretic perspective, and identify challenges for single-task pruning to function effectively for multi-task pruning. We propose Redundancy-Disentangled Networks (RDNeTs), which decouples intra- and inter-redundancy such that all redundancy can be suppressed via previous network pruning schemes. A pruned RDNet also ensures minimal computation in any subset of tasks, a desirable feature for selective task execution. We also propose a heuristic to construct an RDNet from multiple pre-trained networks. Experiments on CelebA (LFW) dataset show that the same pruning method on an RDNet achieves at least  $1.8\times$  ( $1.3\times$ ) lower memory usage and  $1.4\times$  ( $1.8\times$ ) lower computation cost than on a multi-task network constructed by the state-of-the-art network merging scheme.

## References

- [1] Anthony J Bell. The co-information lattice. In *Proceedings of the International Workshop on Independent Component Analysis and Blind Signal Separation: ICA*, 2003.
- [2] Yi-Min Chou, Yi-Ming Chan, Jia-Hong Lee, Chih-Yi Chiu, and Chu-Song Chen. Unifying and merging well-trained deep neural networks for inference stage. In *Proceedings of International Joint Conference on Artificial Intelligence*, pages 2049–2056, 2018.
- [3] Bin Dai, Chen Zhu, Baining Guo, and David Wipf. Compressing neural networks using the variational information bottleneck. In *Proceedings of ACM International Conference on Machine Learning*, pages 1143–1152, 2018.
- [4] Misha Denil, Babak Shakibi, Laurent Dinh, Nando De Freitas, et al. Predicting parameters in deep learning. In *Proceedings of Advances in Neural Information Processing Systems*, pages 2148–2156, 2013.
- [5] Xin Dong, Shangyu Chen, and Sinno Pan. Learning to prune deep neural networks via layer-wise optimal brain surgeon. In *Proceedings of Advances in Neural Information Processing Systems*, pages 4860–4874, 2017.
- [6] Biyi Fang, Xiao Zeng, and Mi Zhang. Nestdnn: resource-aware multi-tenant on-device deep learning for continuous mobile vision. In *Proceedings of ACM Annual International Conference on Mobile Computing and Networking*, pages 115–127, 2018.
- [7] Yiwen Guo, Anbang Yao, and Yurong Chen. Dynamic network surgery for efficient dnns. In *Proceedings of Advances In Neural Information Processing Systems*, pages 1379–1387, 2016.
- [8] Song Han, Xingyu Liu, Huizi Mao, Jing Pu, Ardavan Pedram, Mark A Horowitz, and William J Dally. Eie: efficient inference engine on compressed deep neural network. In *Proceedings of ACM/IEEE Annual International Symposium on Computer Architecture*, pages 243–254, 2016.
- [9] Xiaoxi He, Zimu Zhou, and Lothar Thiele. Multi-task zipping via layer-wise neuron sharing. In *Proceedings of Advances in Neural Information Processing Systems*, pages 6016–6026, 2018.
- [10] Hengyuan Hu, Rui Peng, Yu-Wing Tai, and Chi-Keung Tang. Network trimming: A data-driven neuron pruning approach towards efficient deep architectures. *arXiv preprint arXiv:1607.03250*, 2016.
- [11] Gary Huang, Marwan Mattar, Honglak Lee, and Erik G Learned-Miller. Learning to align from scratch. In *Proceedings of Advances in Neural Information Processing Systems*, pages 764–772, 2012.
- [12] Artemy Kolchinsky and Brendan Tracey. Estimating mixture entropy with pairwise distances. *Entropy*, 19(7):361, 2017.
- [13] Neeraj Kumar, Alexander C Berg, Peter N Belhumeur, and Shree K Nayar. Attribute and simile classifiers for face verification. In *Proceedings of International Conference on Computer Vision*, pages 365–372, 2009.
- [14] Yann LeCun, Léon Bottou, Yoshua Bengio, and Patrick Haffner. Gradient-based learning applied to document recognition. *Proceedings of the IEEE*, 86(11):2278–2324, 1998.
- [15] Hao Li, Asim Kadav, Igor Durdanovic, Hanan Samet, and Hans Peter Graf. Pruning filters for efficient convnets. In *Proceedings of International Conference on Learning Representations*, 2017.

- [16] Ziwei Liu, Ping Luo, Xiaogang Wang, and Xiaoou Tang. Deep learning face attributes in the wild. In *Proceedings of IEEE International Conference on Computer Vision*, pages 3730–3738, 2015.
- [17] Hong Lu, Jun Yang, Zhigang Liu, Nicholas D Lane, Tanzeem Choudhury, and Andrew T Campbell. The jigsaw continuous sensing engine for mobile phone applications. In *Proceedings of ACM Conference on Embedded Network Sensor Systems*, pages 71–84, 2010.
- [18] Rasmus Rothe, Radu Timofte, and Luc Van Gool. Deep expectation of real and apparent age from a single image without facial landmarks. *International Journal of Computer Vision*, 126(2-4):144–157, 2018.
- [19] Andrew Michael Saxe, Yamini Bansal, Joel Dapello, Madhu Advani, Artemy Kolchinsky, Brendan Daniel Tracey, and David Daniel Cox. On the information bottleneck theory of deep learning. In *Proceedings of International Conference on Learning Representations*, 2018.
- [20] Karen Simonyan and Andrew Zisserman. Very deep convolutional networks for large-scale image recognition. *arXiv preprint arXiv:1409.1556*, 2014.
- [21] Vivienne Sze, Yu-Hsin Chen, Tien-Ju Yang, and Joel S Emer. Efficient processing of deep neural networks: A tutorial and survey. *Proceedings of the IEEE*, 105(12):2295–2329, 2017.
- [22] Naftali Tishby and Noga Zaslavsky. Deep learning and the information bottleneck principle. In *Proceedings of IEEE Information Theory Workshop*, pages 1–5, 2015.
- [23] Simon Vandenhende, Bert De Brabandere, and Luc Van Gool. Branched multi-task networks: deciding what layers to share. *arXiv preprint arXiv:1904.02920*, 2019.
- [24] Yi Wang, Jialiu Lin, Murali Annaram, Quinn A Jacobson, Jason Hong, Bhaskar Krishnamachari, and Norman Sadeh. A framework of energy efficient mobile sensing for automatic user state recognition. In *Proceedings of ACM Annual International Conference on Mobile Systems, Applications, and Services*, pages 179–192, 2009.
- [25] Satoshi Watanabe. Information theoretical analysis of multivariate correlation. *IBM Journal of research and development*, 4(1):66–82, 1960.
- [26] Wei Wen, Chunpeng Wu, Yandan Wang, Yiran Chen, and Hai Li. Learning structured sparsity in deep neural networks. In *Proceedings of Advances In Neural Information Processing Systems*, pages 2074–2082, 2016.
- [27] Jason Yosinski, Jeff Clune, Yoshua Bengio, and Hod Lipson. How transferable are features in deep neural networks? In *Proceedings of Advances in Neural Information Processing Systems*, pages 3320–3328, 2014.
- [28] Yu Zhang and Qiang Yang. An overview of multi-task learning. *National Science Review*, 5(1):30–43, 2017.

## Appendix

### A Definitions and Derivations

#### A.1 Vertices in Neural Network Graph

The vertex set  $V$  of a neural network graph  $G$  contains sink, source and internal nodes:

- A source node  $v^x \in \{v|v \in V \wedge \deg^-(v) = 0\}$  represents an input neuron. Each of them outputs a random variable  $X_i \in \mathbf{X}$ . The set of all the source node  $v^x$  outputs the input random variable set  $\mathbf{X}$
- An internal node  $v_i \in \{v|v \in V \wedge \deg^-(v) \neq 0 \wedge \deg^+(v) \neq 0\}$  represents a neuron that calculate the weighted sum of its inputs and then apply an activation function as output:  $T_i = \sigma(\tilde{\mathbf{w}}^\top \tilde{\mathbf{T}}^{in} + b)$ , where  $\tilde{\mathbf{T}}^{in}$  is the input vector, which contains all the outputs of the in-coming neighbours,  $\tilde{\mathbf{w}}$  is the weight vector of the neuron,  $b$  is the bias, and  $\sigma(\cdot)$  is the activation function.
- A sink node  $v^A \in \{v|v \in V \wedge \deg^+(v) = 0\}$  represents a task  $A$ . The input of a sink node is a random variable set  $\hat{\mathbf{Y}}^A$ , which is used as a prediction of  $\mathbf{Y}^A$ . Each sink node corresponds to an individual task.

#### A.2 Layers in Neural Network Graph

We can organise a neural graph  $G$  with a source node set  $\mathbf{v}^x$  and a sink node set  $\mathbf{v}^Y$  into layers  $\Gamma_i$  by Algorithm 2. Note that  $N^+(\mathbf{v})$  represents the out-coming neighbourhood of the vertex set  $\mathbf{v}$ .

---

**Algorithm 2:** Construct Layers

---

**Input:** A neural graph  $G$  with

**Output:**  $N$  layers  $\Gamma_i$  with  $i = 1, \dots, N$ .

```
1  $\Gamma_0 \leftarrow \mathbf{v}^x$ ;  
2  $i \leftarrow 0$ ;  
3 while  $N^+(\Gamma_i) \neq \mathbf{v}^Y$  do  
4    $\Gamma_{i+1} \leftarrow \emptyset$ ;  
5   for each node  $v_i \in \Gamma_i$  do  
6     if  $N^+(v_i) \cap \mathbf{v}^Y \neq \emptyset$  then  
7        $\Gamma_{i+1} \leftarrow \Gamma_{i+1} \cup \{v_i\}$ ;  
8     end  
9   end  
10   $\Gamma_{i+1} \leftarrow \Gamma_{i+1} \cup (N^+(\Gamma_i) \setminus \Gamma_{i+1})$ ;  
11   $i \leftarrow i + 1$ ;  
12 end  
13  $N \leftarrow i$ ;
```

---

### A.3 Derivation of Eq.(4)

The redundancy of the join of two output sets  $\mathbf{T}^1$  and  $\mathbf{T}^2$  can be calculated by:

$$\begin{aligned}
\mathcal{R}_A(\mathbf{T}^1 \cup \mathbf{T}^2) &= \sum_{T_i \in \mathbf{T}^1 \cup \mathbf{T}^2} H(T_i) - I(\mathbf{T}^1, \mathbf{T}^2; \mathbf{Y}^A) \\
&= \sum_{T_i \in \mathbf{T}^1 \cup \mathbf{T}^2} H(T_i) - \left( H(\mathbf{T}^1, \mathbf{T}^2) - H(\mathbf{T}^1, \mathbf{T}^2 | \mathbf{Y}^A) \right) \\
&= \sum_{T_i \in \mathbf{T}^1} H(T_i) + \sum_{T_i \in \mathbf{T}^2} H(T_i) - \sum_{T_i \in \mathbf{T}^1 \cap \mathbf{T}^2} H(T_i) \\
&\quad - \left( H(\mathbf{T}^1) + H(\mathbf{T}^2) - I(\mathbf{T}^1; \mathbf{T}^2) \right) \\
&\quad + \left( H(\mathbf{T}^1 | \mathbf{Y}^A) + H(\mathbf{T}^2 | \mathbf{Y}^A) - I(\mathbf{T}^1; \mathbf{T}^2 | \mathbf{Y}^A) \right) \\
&= \mathcal{R}_A(\mathbf{T}^1) + \mathcal{R}_A(\mathbf{T}^2) + I(\mathbf{T}^1; \mathbf{T}^2) - I(\mathbf{T}^1; \mathbf{T}^2 | \mathbf{Y}^A) - \sum_{T_i \in \mathbf{T}^1 \cap \mathbf{T}^2} H(T_i) \\
&= \mathcal{R}_A(\mathbf{T}^1) + \mathcal{R}_A(\mathbf{T}^2) + I(\mathbf{T}^1; \mathbf{T}^2; \mathbf{Y}^A) - \sum_{T_i \in \mathbf{T}^1 \cap \mathbf{T}^2} H(T_i)
\end{aligned}$$

### A.4 Derivation of Eq.(5)

For simplicity we denote  $\mathcal{R}_A(\mathbf{T}^1 \cup \mathbf{T}^2)$  by  $\mathcal{R}_A(\mathbf{T}^1, \mathbf{T}^2)$ . According to Eq.(4), we have

$$\begin{aligned}
\mathcal{R}_A(G^A) &= \mathcal{R}_A(\mathbf{L}_1^A, \dots, \mathbf{L}_N) \\
&= \mathcal{R}_A(\mathbf{L}_1^A, \dots, \mathbf{L}_{N-1}) + \mathcal{R}_A(\mathbf{L}_N) + I(\mathbf{L}_N; \mathbf{Y}^A) - \sum_{T_i \in \mathbf{L}_{N-1} \cap \mathbf{L}_N^A} H(T_i) \\
&\quad \vdots \\
&= \sum_{i=1}^N \mathcal{R}_A(\mathbf{L}_i^A) + \sum_{i=2}^N I(\mathbf{L}_i^A; \mathbf{Y}^A) - \sum_{i=2}^N \sum_{T_i \in \mathbf{L}_{i-1}^A \cap \mathbf{L}_i^A} H(T_i) \\
&= \sum_{i=1}^N \left( \mathcal{R}_A(\mathbf{L}_i^A) - \sum_{T_i \in \mathbf{L}_{i-1}^A \cap \mathbf{L}_i^A} H(T_i) \right) + \sum_{i=2}^N I(\mathbf{L}_i^A; \mathbf{Y}^A)
\end{aligned}$$

## B Implementation Details

### B.1 CelebA

We divide the dataset into training and test sets containing 80% and 20% of the samples. The input picture resolution is resized to  $72 \times 72$  and the width of the fully connected layers in VGG-16 is changed to 512. The convolutional layers are initialised with weights pre-trained for imdb-wiki [18], and use the same pre-processing steps. The baselines and RDNet are pruned via VIB: First 30 Epochs with KL-factor set to  $1 \times 10^{-5}$ , then 10 Epochs with KL-factor  $1 \times 10^{-6}$ .

### B.2 LFW

The dataset is divided into training and test sets containing 80% and 20% of the samples. Same as in CelebA, the input picture resolution is resized to  $72 \times 72$  and the width of the fully connected layers in VGG-16 is changed to 512. The convolutional layers are initialised with weights pre-trained for imdb-wiki [18], and use the same pre-processing steps. The baselines and RDNet are pruned via VIB: First 120 Epochs with KL-factor set to  $4 \times 10^{-5}$ , then 40 Epochs with KL-factor  $1 \times 10^{-6}$ .